JOURNAL OF MATERIALS SCIENCE 26 (1991) 28–34

High-temperature deformation characteristics of Ti–15 at. % Al alloy

K. NIIMI, K. MORII, Y. NAKAYAMA
College of Engineering, University of Osaka Prefecture, Mozu-Umemachi, Sakai 591, Japan

The deformation characteristics of Ti–15 at. % Al alloy have been investigated by compression tests in the temperature range 873 to 1273 K (0.44 to 0.64 T_m) and by extensive transmission electron microscopy. Two types of deformation patterns were identified depending on the temperature: at lower temperatures below about 1073 K, the yield stress of the sample showed inverse temperature dependence, and serrations were found on the flow curves, whereas the normal dependences of the yield stress on temperature and strain rate were found at higher temperatures above about 1073 K. Corresponding dislocation substructures were composed of coarse bands of localized slip at 1023 K, and of rather uniformly distributed dislocations at 1123 K, and sub-boundaries as well as free dislocations at 1273 K. The main operating mechanisms in these temperature regimes were assumed to be the co-operative movement of numerous dislocations under the condition of the dynamic strain ageing, viscous glide of dislocations and dynamic recovery, respectively.

1. Introduction

Commercial titanium alloys designed for high-temperature applications are usually composed of α (h c p) phase, because no phase transformations occur during exposure at a service temperature. The α-alloys commonly contained relatively high concentrations of aluminium as a basic alloying element, which contributes to stabilization and solid-solution strengthening of the α-phase [1]. Some additional elements, such as tin, zirconium, niobium and silicon, are also added to improve microstructure and high-temperature properties [1].

In α-Ti–Al alloys with an aluminium concentration more than about 10 at. %, ordered particles of Ti_3Al (α_2) phase with the hexagonal DO_{19} structure precipitate upon ageing [2, 3]. The presence of the α_2-particles within the α-phase tended to reduce the room-temperature ductility and to increase the susceptibility to stress-corrosion cracking [4, 5]. Accordingly, the aluminium content in most commercial alloys is controlled at less than about 10 at. %. Recent investigations on an aged commercial alloy (Ti–8Al–5Nb–5Zr–0.25Si), however, showed that a fine dispersion of the α_2-particles can improve significantly the mechanical properties at elevated temperature [6]. The result suggests that the high-temperature plastic behaviour of the α-titanium alloys is closely correlated with the ordered α_2-particles; detailed investigation of the alloys with high aluminium concentrations still seems to be valuable for the development of high-temperature titanium alloys.

The aim of the present work was to study the temperature dependence of yield stress and microscopic deformation modes in a Ti–Al binary alloy with 15 at. % Al at high temperature. According to the Ti–Al phase diagram [2, 3], the composition of the present alloy lies within the ($\alpha + \alpha_2$) two-phase field from room temperature to about 1073 K and in the single-phase field of α at a temperature about 1073 and 1323 K. This paper reports some experimental results on deformation modes and dislocation substructure in the solution-treated Ti–15 at. % Al alloy which was strained by compression in a temperature range between 873 and 1273 K (0.44 to 0.64 T_m, where T_m is the melting point in K); the results on the aged alloy containing the α_2 particles will be described separately.

2. Experimental procedure

A small ingot (about 500 g) with a nominal composition of Ti–15 at. % Al was produced from appropriate amounts of high-purity aluminium (99.99%) and titanium (99.9%) by a vacuum arc-melting technique, and was forged into a slab 5 mm thick at 1473 K. Chemical analysis showed the aluminium content of the slab to be 14.9 at. % (9.1 wt %). Small rectangular blocks for compression tests were cut to a size of about 3 mm × 3 mm × 5 mm using a SiC blade cutter. Samples were prepared by annealing these blocks in a vacuum furnace for 8 h at 1300 K, just below the β-transus of the alloy, and by subsequent water quenching after breaking the vacuum. An optical observation indicated that the heat-treated samples were composed of a single phase of α-titanium with large equiaxed grains of about 200 μm diameter. No apparent preferred orientations were found by X-ray pole figure measurements. Prior to deformation, all the rectangular samples were abraded with emery

0022–2461/91 $03.00 + .12

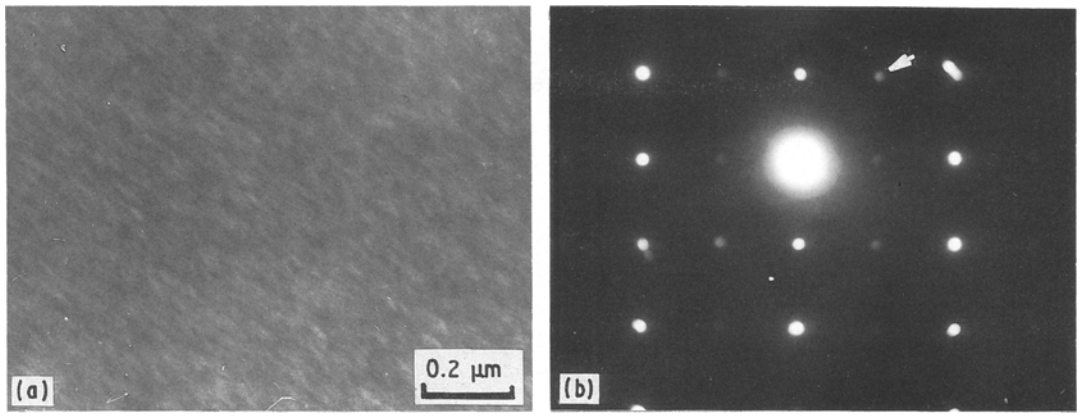

Figure 1 Electron microstructure of undeformed Ti–15 at. % Al alloy: (a) dark-field micrograph taken using a superlattice spot (0 1 $\bar{1}$ 1) (arrow), and (b) corresponding selected-area diffraction pattern, showing the presence of fine Ti_3Al (α_2) particles.

paper to make their two facing planes parallel and were finished by electrolytic polishing.

The stress–strain relation of the Ti–15 at.% Al alloy at high temperature was evaluated by uniaxial compression with an Instron-type machine. The compression tests were performed under high vacuum of about 1×10^{-5} torr (1 torr = 133.322 Pa) at several temperatures between 873 and 1273 K, and at constant cross-head speeds, corresponding to the strain rates of 1×10^{-3}, 3×10^{-3} and 1×10^{-2} sec^{-1}. The samples were heated by a r.f. induction apparatus during deformation, and the temperature was controlled with the help of an optical sensor. The samples were held at a given temperature of deformation for 20 min before starting the compression test so as to attain as much phase equilibrium as possible.

The microscopic deformation pattern of the alloy was investigated by a transmission electron microscope operating at 100 kV. Thin foils for this observation were prepared by a conventional method [7] from the slices cut parallel to the compression axis of the deformed samples.

3. Results

3.1. Initial microstructure

The optical microstructure of the undeformed sample, which was subjected to the solution treatment at 1300 K followed by water quenching, heating to a testing temperature, and to furnace cooling, consisted of the single-phase α. Transmission electron microscopy (TEM) on this sample, however, showed the presence of very fine particles of the α_2-phase within the α-grains, as indicated in Fig. 1. The selected-area diffraction (SAD) pattern contained several superlattice spots due to the α_2-phase (Fig. 1b). The dark-field image obtained with the superlattice spot exhibited homogeneously distributed fine α_2-particles (Fig. 1a). Lütjering and Weissmann [8] have observed a similar microstructure in Ti–14 to 18 at. % Al alloys quenched from 973 to 1273 K, and have shown that the α_2-particles could be formed during quenching, and were distributed uniformly with an average diameter of 2 nm and a volume fraction of about 0.03 %: the precipitation of the α_2-particles is hard to suppress by a conventional quenching technique. Nevertheless, the undeformed sample could be regarded roughly as a solid solution, because the number of precipitated α_2-particles seems to be quite a few (Fig. 1).

3.2. Mechanical behaviour at high temperature

Typical examples of the flow curves obtained by the compression test at the strain rate of 1×10^{-3} sec^{-1} are shown in Fig. 2. Within the temperature range employed, all the samples exhibited parabolic strain hardening, and the hardening rate gradually decreased with increasing deformation temperature. Two different shapes of the flow curves were identified depending on the temperature of deformation: the samples tested in a temperature range 873 to 1023 K exhibited serrations on their flow curves, whereas those tested at a temperature higher than about 1073 K deformed with a smooth flow curve, as seen

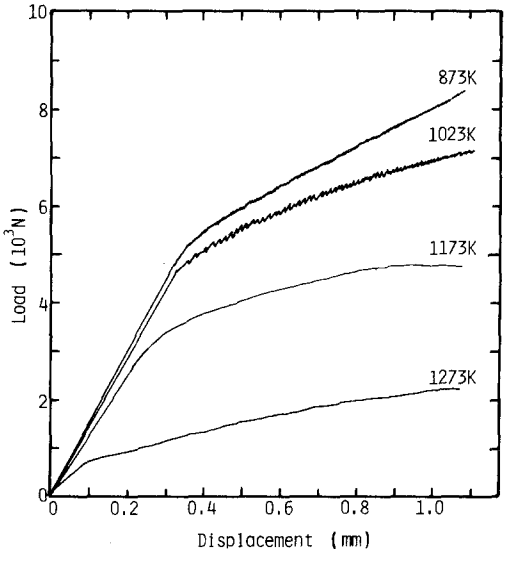

Figure 2 Flow curves obtained by compression tests of Ti–15 at. % Al alloy at the temperature indicated (strain rate = 1×10^{-3} sec^{-1}).

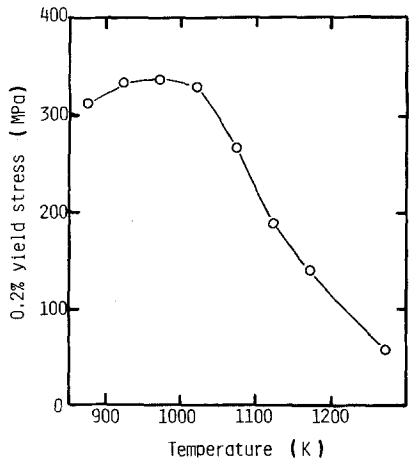

Figure 3 0.2% offset yield stress of Ti–15 at. % Al alloy as a function of temperature of deformation (strain rate = 1×10^{-3} sec^{-1}).

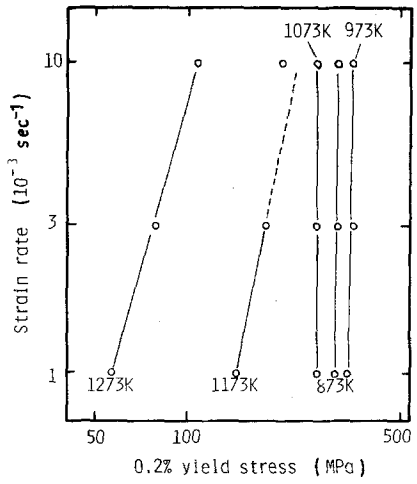

Figure 4 Strain-rate dependence of the yield stress of Ti–15 at. % Al alloy. The slope of least-square plots gave n-values of 5.4 at 1173 K and 3.5 at 1273 K.

from Fig. 2. The result suggests that different deformation mechanisms were operating in both two-temperature regimes; hereafter these will be referred to as the intermediate- (873 to 1073 K) and high-temperature range (1073 to 1273 K). Here, it is interesting to note that these two ranges correspond, respectively, to the two-phase ($\alpha + \alpha_2$) and single-phase (α) fields on the phase diagram [2, 3].

In accordance with such a characterization of the deformation temperature, two different features were found in the change in the yield stress with temperature and strain rate. The 0.2% offset yield stress is plotted as a function of the deformation temperature in Fig. 3, and the effect of the strain rate on the yield stress is given in Fig. 4. In the intermediate-temperature range where the serrated flow appeared (Fig. 1), the yield stress increased slightly as the temperature increased (Fig. 3), manifesting itself in the appearance of the inverse temperature dependence of the yield stress in the present alloy. This behaviour was found during deformation at a strain rate less than about 1×10^{-2} sec^{-1}. In addition, the yield stress was almost independent of strain rate (Fig. 4); in a limited case, the yield stress was found to increase slightly when the strain rate was reduced to 3×10^{-4} sec^{-1}.

In contrast, in the high-temperature range, the yield stress decreased steeply as the deformation temperature increased, and rose with increasing strain rate (Figs 3 and 4), indicating a normal dependence of the yield stress on temperature as well as on strain rate. The stress exponent in the equation $\dot{\varepsilon} = A\sigma^n$ was calculated to be about 5.4 and 3.5 from the slope of the least-square plots of the data at 1173 and 1273 K, respectively.

3.3. Slip bands and dislocation substructure

The macroscopic deformation modes of the samples also showed two different patterns depending on the deformation temperature as indicated in Fig. 5. In the intermediate-temperature range, 873 to 1073 K, the slip bands observed on α-grains were rather straight and coarse. As the deformation temperature increased up to 1123 to 1273 K in the high-temperature range, the slip bands were replaced by a homogeneous pattern, and resulted in fine slip bands. The effect of the strain rate on the slip-band pattern was barely seen due mainly to the limited range of strain rate employed.

TEM observation of the samples strained up to

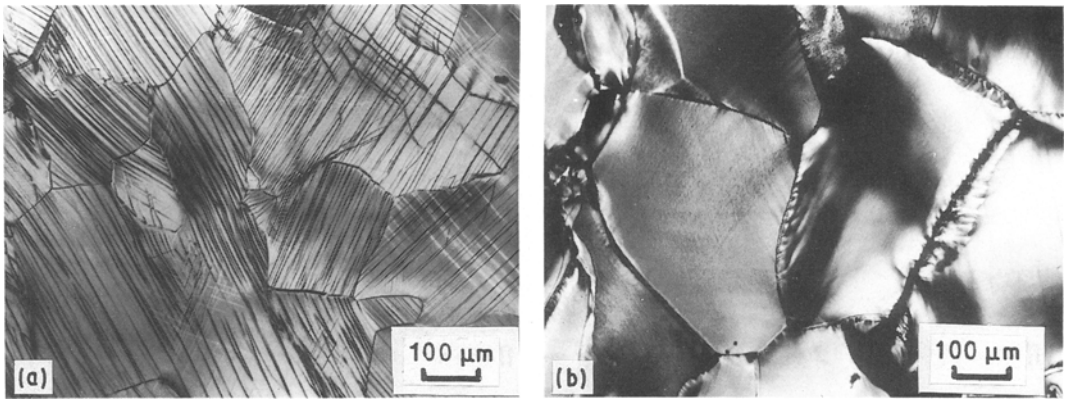

Figure 5 Macroscopic slip bands of Ti–15 at. % Al alloy deformed by compression at (a) 1023 K ($\varepsilon = 1.7\%$) and (b) 1273 K ($\varepsilon = 1.0\%$).

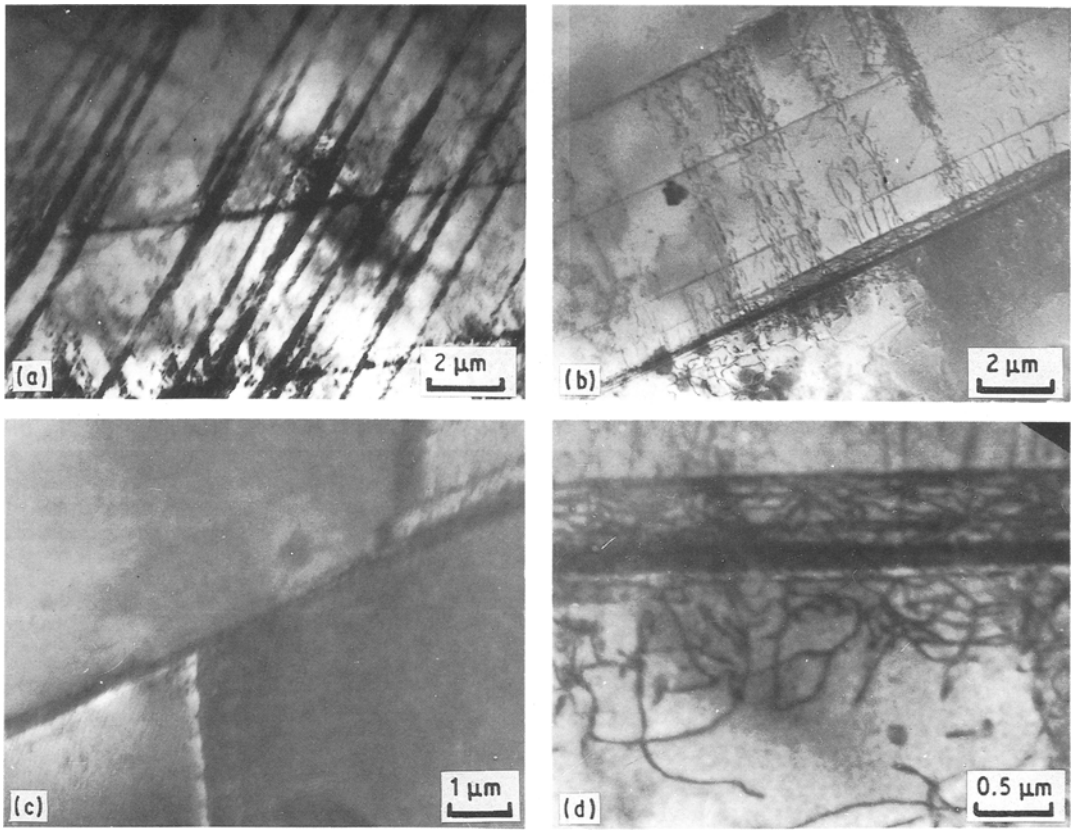

Figure 6 Transmission electron micrographs of Ti–15 at. % Al alloy deformed 1.7% by compression at 1023 K, showing bands of localized slip on (a) prismatic planes (a) and (b) basal planes. Large shear produced within a band and dislocation substructure of the band are shown in (c) and (d), respectively.

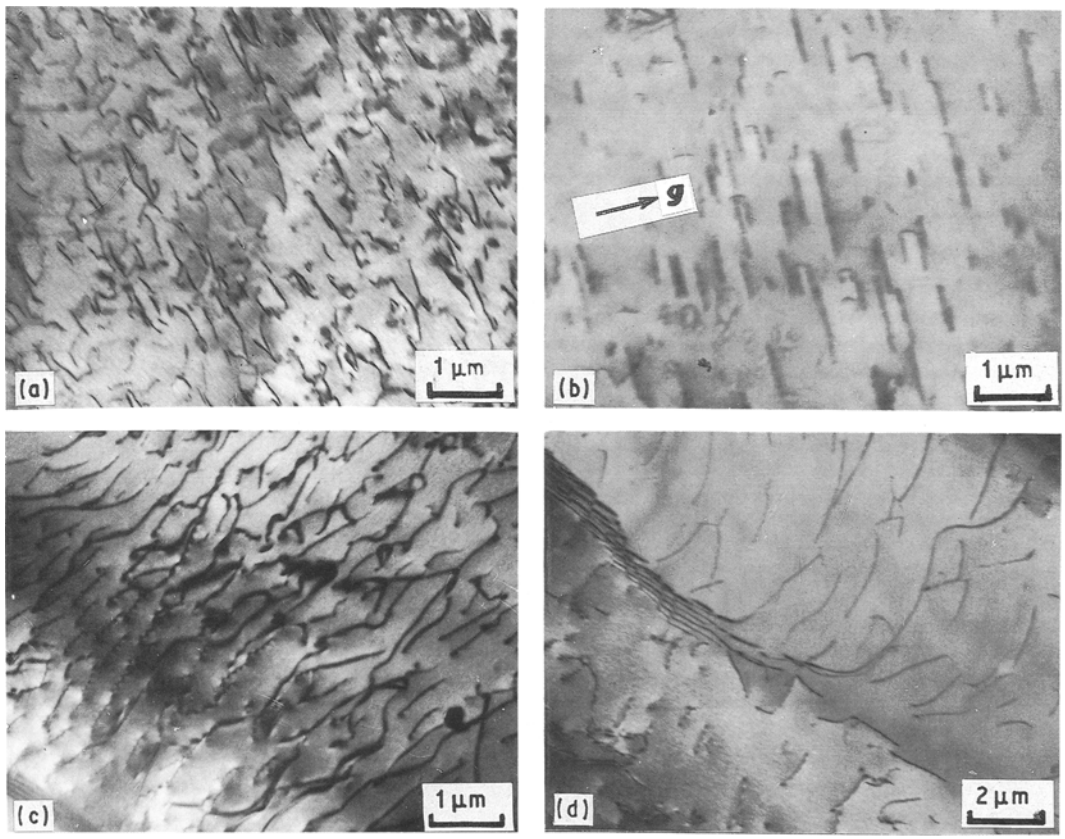

Figure 7 Transmission electron micrographs of Ti–15 at. % Al alloy deformed 1% by compression at (a, b) 1123 K and (c, d) 1273 K, showing (a, c) uniform distribution of dislocations, (b) non-$\langle a \rangle$-type dislocations ($\boldsymbol{g} = 0\,0\,0\,2$), and (d) formation of sub-boundary.

about 3% was carried out to identify the microscopic modes of deformation; some examples are shown in Figs 6 and 7. The microscopic deformation modes were in accord with the optical observation given in Fig. 5. The compressive deformation in the intermediate-temperature range produced coarse bands of localized slip parallel to the prismatic or basal planes. Although the width of the bands is narrow ($< 0.2\,\mu m$), they extended almost over a whole grain and produced intense localized shear in the band. A large number of dislocations were formed and trapped within the bands, which is attributed to the occurrence of the large localized shear. In a region between two adjacent slip bands, only a few dislocations were activated at low strains. With increasing strain, such a slip-band pattern remained basically unchanged, but the dislocation density increased rapidly in the regions between the bands.

In contrast to the localized slip mode in the temperature range 873 to 1073 K, the deformation in the high-temperature range, 1073 to 1273 K, was characterized by a uniform distribution of dislocations and by sub-boundaries, as shown in Fig. 7. The dislocation substructure observed at 1123 K was composed of randomly distributed dislocation segments with rather irregular shapes. The dislocations having the $\langle a \rangle$-type Burgers vector, $a/3\langle 1\,1\,\bar{2}\,0 \rangle$, were dominant, while non-$\langle a \rangle$-type dislocations were also detected in grains with a suitable orientation. Deformation at a higher temperature such as 1273 K altered slightly the dislocation arrangement: relatively long free dislocations with the screw component and sub-boundaries constructed by edge segments were observed, indicating frequent cross-slip of screw dislocations.

4. Discussion

Two outstanding deformation features were identified in the present Ti–15 at. % Al alloy depending on the testing temperature. A correlation between the operating deformation modes and dislocation substructures is briefly examined based on the observed results.

4.1. Intermediate-temperature range (873 to 1073 K)

In this temperature range the deformation mode was characterized by the appearance of the inverse temperature dependence of the yield stress and of the serrations (Figs 1 and 2). The coarse bands of localized slip observed by TEM (Fig. 6) seem to be closely connected to the onset of the serrated flow. The formation of such bands may be responsible for a collective movement of a large number of dislocations, including their co-operative multiplication and propagation, on limited slip planes, which could be triggered either by overcoming local obstacles by dislocations, or by the breakdown of some kinds of barriers for the dislocation motion [9, 10], as discussed below.

The serrated flow observed had the following features: most of the serrations were found to begin immediately after yielding and continued up to a strain of about 20%. The occurrence of the serrations was dependent on the strain rate; the serrated flow was hardly detected at a strain rate of $1 \times 10^{-2}\,sec^{-1}$. In addition, the amplitude and frequency of the serrations were increased as the temperature increased from 873 to 1023 K (Fig. 1). Very similar serrations have been observed on Ti–Al alloys by Rosenberg and Nix [11], and on Ti–5 Al–2.5 Sn alloys by Döner and Conrad [12]. They have attributed the serrations in these materials to the effects of the substitutional solute atoms, aluminium and/or tin (dynamic strain ageing or the Poretvin–LeChatelier effect). The possibility of this effect being due to interstitial atoms such as oxygen, has been considered to be low from the discussion of their activation energy for diffusion [12]. Accordingly, the contribution of aluminium atoms to the serrated flow could also be assumed to be important in the present alloy. Because the temperature range of the compression tests is within the $(\alpha + \alpha_2)$ field, the atmospheres or clusters of aluminium atoms are likely to be formed by strain ageing on to moving as well as stationary dislocations during deformation. This process could lead to an increase in the strength of obstacles and to a locking of some fraction of mobile dislocations. Unlocking of aged dislocations or overcoming the local obstacles by dislocations will act as a trigger for the collective motion of numerous dislocations, which could result in an unstable flow [13]. The strength of the locking due to the solute atmosphere will increase, more or less, as the ageing temperature, i.e. the deformation temperature rises to an appropriate temperature; this seems to be a cause for the inverse temperature dependence of the yield stress of the present alloy.

In addition, the presence of the fine ordered particles of α_2 formed during the quenching process may also provide an additional trigger for the unstable flow, because local shearing of the coherent particles by the dislocations tends to yield the local softening of the slip plane over which the dislocations swept out, as observed in Ni–Ni_3Al [14] and Al–Li_3Al [15] systems. In this case, the inverse temperature dependence of the yield stress is attributable to that of the ordered particles.

4.2. High-temperature range (1073 to 1273 K)

In this temperature range where only the single-phase of α-titanium is stable, the compression tests showed marked dependence of the yield stress on both the deformation temperature and strain rate (Figs 2 and 3). Because the temperature of deformation is high enough for the diffusion of aluminium atoms, the solute atmosphere, which seems to be almost in thermal equilibrium, will be formed around the moving dislocations, and can move with the dislocations by diffusion. This gives rise to a viscous resistance to the dislocation motion which provides the normal dependence of the yield stress on temperature and strain rate [16, 17].

Although the yield stress decreased simply with increasing temperature in this temperature range (Fig. 2), the dislocation substructures observed by

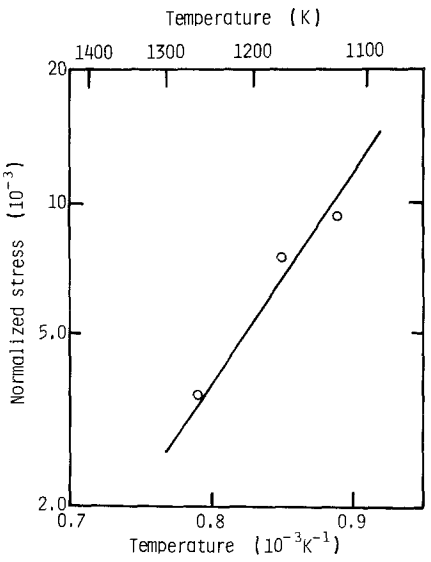

Figure 8 Normalized yield stress ($\ln(\sigma/G)$, G = shear modulus) as a function of temperature ($1/T$) in the Arrhenius-plot for Ti–15 at. % Al alloy deformed by compression in the temperature range 1123 to 1273 K.

TEM were somewhat different depending on the temperature tested, suggesting a slight change in the operating mechanism with increasing temperature. At a lower temperature such as 1123 K a rather uniform distribution of dislocations was observed, whereas many free dislocations and well-defined sub-boundaries were typical at a higher temperature of 1273 K (Fig. 7). The former suggests that the presence of friction stress for dislocation motion, and hence viscous glide of dislocations caused by dragging the solute atmosphere seems to be a major operating mechanism. Similar observations have been made on several alloys whose deformation is controlled by the dragging mechanism [18, 19]. The latter may indicate the result of a strong contribution of recovery processes with increasing deformation temperature. It is possible, for example, to ascribe this behaviour to the cross-slip of screw segments from prismatic to basal planes, and to form sub-boundaries by edge segments left behind on the prismatic planes.

An apparent stress exponent in the equation $\dot{\varepsilon} = A\sigma^n$ was estimated to be about 5.4 and 3.5 at 1173 and 1273 K, respectively (Fig. 4). Similar results have been obtained by Oikawa and Oomori on Ti–1 to 7 mol % Al alloys [20]. They showed that the stress exponent, n, could change from 3.5 to 4.6 with increasing stress level imposed. Then, the value of n, 5.4, of the present alloy at 1173 K is supposed to decrease slightly as the strain rate was reduced below 1×10^{-3} sec^{-1}. If we assume the following equation for high-temperature creep to be applicable for the present case, $\dot{\varepsilon} = A(\sigma/G)^n \exp(-Q/RT)$ [21], where $\dot{\varepsilon}$ is steady-state creep rate, A a constant, (σ/G) the normalized stress by the shear modulus G, RT has its normal meaning, an apparent activation energy for deformation, Q, can be estimated by the plot of $\ln(\sigma/G)$ against $1/T$: the present results in the temperature range 1223 to 1273 K at 1×10^{-3} sec^{-1} are plotted in Fig. 8. From the least-square slope, $Q = 290\,kJ\,mol^{-1}$, the apparent activation energy for deformation, was obtained for $n = 3.5$, which is close to that obtained by Oikawa and Oomori [20]. However, this is rather a high value compared with that of self diffusion, D, of α-titanium ($D = 169\,kJ\,mol^{-1}$ [22]) or of impurity diffusion of aluminium in Ti–Al alloy ($D = 156\,kJ\,mol^{-1}$ [23]). A similar trend was commonly observed in materials with the h c p structure [17]. According to the present TEM results, of the many mechanisms proposed to explain this behaviour, the cross-slip model [19] seems to be important for the present alloy deformed at a high temperature such as 1273 K.

5. Conclusion

The Ti–15 at. % Al alloy strained by compression in the temperature range between 873 and 1273 K showed two characteristic deformation modes depending on the temperature. Although the macroscopic deformation pattern showed a remarkable difference, the microscopic operating mechanisms responsible for these deformation modes were able to be correlated with the change in the method of interaction between the solute atoms of aluminium and dislocations with increasing temperature.

It is noted with regard to the high-temperature strength of titanium alloys that the present alloy showed rather high yield stress up to about 1073 K compared with that of a typical α-alloy such as Ti–5Al–2.5Sn [12], and followed by a significant decrease in the yield stress (Fig. 2). From practical viewpoints, the former may give information on the strengthening due to high solute contents, and the latter on the formability of the alloy.

References

1. M. PETERS, *Metall.* **37** (1983) 584.
2. M. J. BLUCKBURN, *Trans. Met. Soc. AIME* **239** (1967) 1200.
3. T. K. G. NAMBOODHIRI, C. J. McMAHON and H. HERMAN, *Met. Trans.* **4** (1973) 1323.
4. M. J. BLACKBURN and J. C. WILLIAMS, *Trans. ASM* **62** (1969) 398.
5. T. R. BECK, *J. Electrochem. Soc.* **114** (1967) 551.
6. C. G. RHODES, N. E. PATON and M. W. MAHONEY, in "Titanium Science and Technology", edited by G. Lutjering, U. Zwicker and W. Bunk (Deutsche Gesellschaft für Metallkunde, Oberusel, 1985) p. 2355.
7. R. A. A. SPRLING, *Met. Trans.* **6A** (1975) 1660.
8. G. LÜTJERING and S. WEISSMANN, *Acta Metall.* **18** (1970) 785.
9. T. TABATA, H. FUJITA and Y. NAKAJIMA, *ibid.* **28** (1980) 795.
10. F. MONCHOUX and H. NEUHÄUSER, *J. Mater. Sci.* **22** (1987) 1443.
11. H. W. ROSENBERG and W. D. NIX, *Met. Trans.* **4** (1973) 1333.
12. M. DÖNER and H. CONRAD, *Met. Trans.* **6A** (1975) 853.
13. S. SCHOECK, *Acta Metall.* **32** (1984) 1229.
14. S. M. COPLY and B. H. KEAR, *Trans. Met. Soc. AIME* **239** (1967) 977.
15. M. TAMURA, T. MORI and T. NAKAMURA, *Trans. Jpn Inst. Metals* **14** (1973) 354.
16. S. M. L. SASTRY, P. S. PAO and K. K. SANKARAN, in "Titanium '80 Science and Technology", edited by A. Kimura

and O. Izumi (Metallurgical Society of AIME, Warrendale, Pennsylvania, 1980) p. 873.
17. H. SIETHOFF and K. AHLBORN, *Z. Metallkde* **76** (1985) 627.
18. R. HORIUCHI and M. OTSUKA, *J. Jpn Inst. Metals* **35** (1971) 406.
19. S. S. VAGARALI and T. G. LANGDON, *Acta Metall.* **30** (1982) 1157.
20. H. OIKAWA and T. OOMORI, *Mater. Sci. Engng* **A104** (1988) 125.
21. A. K. MUKHERJEE, J. E. BIRD and J. E. DORN, *Trans. ASM* **62** (1969) 155.
22. J. RAISANEN, *J. Appl. Phys.* **57** (1985) 613.
23. F. DYMENT, in "Titanium '80 Science and Technology", edited by H. Kimura and O. Izumi (Metallurgical Society of AIME, Warrendale, Pennsylvania, 1980) p. 519.

Received 18 August 1989
and accepted 19 February 1990